

# Response of Retaining Wall to Support OB Dump under Active Earth Pressure Using Limit Equilibrium Method

<sup>[1]</sup> Chidanand M Jadar, <sup>[2]</sup> K Madhan Mohan Reddy, <sup>[3]</sup> Jyothi M T

<sup>[1]</sup> Assistant Professor, <sup>[2][3]</sup> UG student

<sup>[1][2][3]</sup> Civil Engineering Department, Acharya institute of Technology, Bangalore, India.

**Abstract:** Retaining walls are the most common structures which are used to support the backfill. These structures are often seen at road and railway embankments, construction of residential and civil buildings and etc. In recent days, retaining walls are also constructed to hold back the soil of mine over burden dumps. In the present study, a 5m retaining wall is analyzed against active earth pressure. The wall is assumed to be vertical with rough surface. Soil parameters like cohesion, adhesion, angle of internal friction of soil are considered. Normally the density of OB dumps is noticed to be higher than that of regular density of soil what is considered in traditional analysis of the retaining wall. Hence, an augmented weight portions are considered in the present analysis. Failure surface is varied by changing the values of rupture surface angles. Using limit equilibrium method, equations to determine active earth pressure is derived. Simplex iteration technique is used to optimize the equation of active earth pressure. A detailed parametric study shows the variation of coefficient of active earth pressure against the variation of parameters like friction angle, cohesion, and adhesion and unit weight of soil. A sensitivity analysis is also done for the behavior of rupture surface by changing different soil parameters.

**Keywords:** Over Burden Dumps, Retaining walls, Limit equilibrium method, Optimization.

## I. INTRODUCTION

Analytical works on earth pressure coefficients for retaining walls started by Rankine(1857) and Coulomb(1776). Coulomb(1776) had given the solutions for lateral earth pressure under the consideration of homogenous and isotropic soil with cohesionless and plane rupture surface. Rankine(1857) also given solution for lateral earth pressure with same considerations. Bell(1915) given equation to encounter the effects of cohesion on the rupture surface. Kapila(1962) and Mononobe and Matsuo(1929) enclosed BIS code (IS1983-1984). Teraghi(1943) considered the log spiral curve as the rupture surface. Prakash and Saran(1966), Saran and Prakash(1968) et al stretched out the coulomb theory by introducing seismic active earth pressure with C- $\phi$  backfill Saran and Gupta(2013) and Ghosh et. al(2008) had discovered the dynamic active earth pressure in C- $\phi$  nature of soil. Ghosh and Saran(2010) and Sharama and Ghosh(2010) had founded the active earth pressure coefficient for single critical wedge angle for variable action of weight, surcharge and cohesion. Ghosh and saran(2010) was found the graphical dynamic earth pressure for C- $\phi$  nature of soil. Recently, Jadar and Ghosh(2017) applied the concepts of retaining wall to solve problem of seismic bearing capacity. Keeping the above facts in view, an approach has been advanced in this paper to get more actual values of active earth pressure using limit equilibrium method.

Also, the outcome of cohesive resistance of soil mass and adhesive capacity of wall surface have been taken into account to optimize the values of is assumed soil mix with mining's having varying density 1.1, 1.2, 1.3 times of natural density of soil.

## ANALYTICAL SOLUTION:

A vertical retaining wall of H meters height is considered for the analysis. The wall is assumed to be supporting soil mixed with mining having varying density 1.1, 1.2, 1.3 times of natural density of soil. Soil parameters like cohesion, adhesion, angle of internal friction of soil and angle of wall friction are accounted. Rupture angle to the vertical are considered as  $\theta$ . Equivalent coefficient of active earth pressure is to be determined under different density cases.

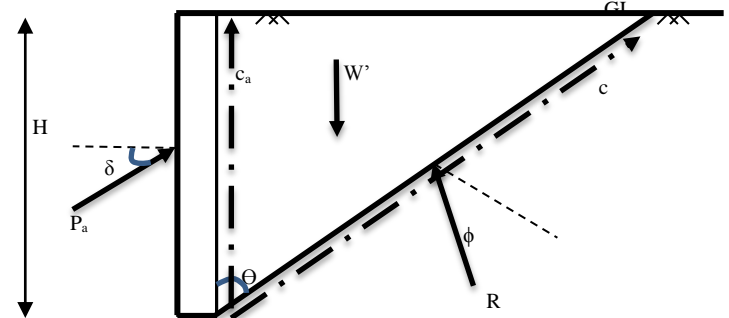


Figure 1. Various forces acting on retaining wall

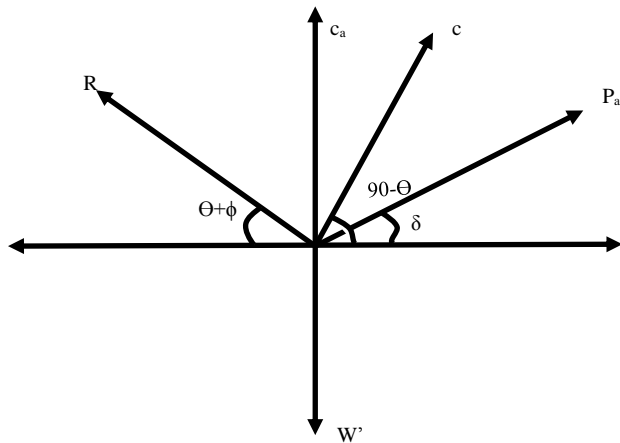


Figure 2. Free body diagram

**DERIVATION OF FORMULATIONS CONSIDERING ACTIVE STATE OF EQUILIBRIUM**

$$\sum H=0$$

$$P_a \cos \delta + c \cos(90 - \theta) = R \cos(\theta + \phi)$$

$$P_a \cos \delta + c \sin \theta = R \cos(\theta + \phi)$$

$$R = \frac{P_a \cos \delta + c \sin \theta}{\cos(\theta + \phi)} \dots \dots \dots \text{Equation (1)}$$

$$\sum V=0$$

$$R \sin(\theta + \phi) + c_a + C \sin(90 - \theta) + P_a \sin \delta = W'$$

$$R \sin(\theta + \phi) + c_a + c \cos \theta + P_a \sin \delta = W' \dots \dots \dots \text{Equation (2)}$$

(2)

Solving equation 1 & 2

$$\left[ \frac{P_a \cos \delta + c \sin \theta}{\cos(\theta + \phi)} \right] \sin(\theta + \phi) + c_a + c \cos \theta + P_a \sin \delta = W'$$

$$P_a \cos \delta \sin(\theta + \phi) + c \sin \theta \sin(\theta + \phi) + c_a \cos(\theta + \phi) + \phi) + c \cos \theta \cos(\theta + \phi) + P_a \sin \delta \cos(\theta + \phi) = W' \cos(\theta + \phi)$$

$$P_a \sin(\theta + \phi + \delta) + C \cos \phi + C_a \cos(\theta + \phi) = W' \cos(\theta + \phi)$$

$$P_a = \frac{W' \cos(\theta + \phi) - C \cos \phi - c_a \cos(\theta + \phi)}{\sin(\theta + \phi + \delta)}$$

$$C = \frac{c \cdot h}{\cos \theta}, C_a = c_a \cdot h, W' = 1.1W = \frac{11}{10} \left( \frac{1}{2} \gamma h^2 \tan \theta \right)$$

$$P_a = \frac{\left[ \frac{11}{10} \left( \frac{1}{2} \gamma h^2 \tan \theta \right) \cos(\theta + \phi) - \left( \frac{c \cdot h}{\cos \theta} \right) \cos \phi - c_a \cdot h \cos(\theta + \phi) \right]}{\sin(\theta + \phi + \delta)}$$

$$P_a = \frac{1}{2} \gamma h^2 \left\{ \left( \frac{11 \tan \theta \cos(\theta + \phi)}{10 \sin(\theta + \phi + \delta)} \right) - \left( \frac{2c \cos \phi}{\gamma h \cos \theta \sin(\theta + \phi + \delta)} \right) - \left( \frac{2c_a \cos \phi}{\gamma h \sin(\theta + \phi + \delta)} \right) \right\}$$

$$K_a =$$

$$\left( \frac{11 \tan \theta \cos(\theta + \phi)}{10 \sin(\theta + \phi + \delta)} \right) - \left( \frac{2c \cos \phi}{\gamma h \cos \theta \sin(\theta + \phi + \delta)} \right) - \left( \frac{2c_a \cos \phi}{\gamma h \sin(\theta + \phi + \delta)} \right)$$

Similarly for \$W'=1.2W\$ and \$W'=1.3W\$ we get,

$$P_a = \frac{1}{2} \gamma h^2 \left\{ \left( \frac{6 \tan \theta \cos(\theta + \phi)}{5 \sin(\theta + \phi + \delta)} \right) - \left( \frac{2c \cos \phi}{\gamma h \cos \theta \sin(\theta + \phi + \delta)} \right) - \left( \frac{2c_a \cos \phi}{\gamma h \sin(\theta + \phi + \delta)} \right) \right\}$$

$$K_a = \left( \frac{6 \tan \theta \cos(\theta + \phi)}{5 \sin(\theta + \phi + \delta)} \right) - \left( \frac{2c \cos \phi}{\gamma h \cos \theta \sin(\theta + \phi + \delta)} \right) - \left( \frac{2c_a \cos \phi}{\gamma h \sin(\theta + \phi + \delta)} \right)$$

$$P_a = \frac{1}{2} \gamma h^2 \left\{ \left( \frac{4 \tan \theta \cos(\theta + \phi)}{3 \sin(\theta + \phi + \delta)} \right) - \left( \frac{2c \cos \phi}{\gamma h \cos \theta \sin(\theta + \phi + \delta)} \right) - \left( \frac{2c_a \cos \phi}{\gamma h \sin(\theta + \phi + \delta)} \right) \right\}$$

$$K_a = \left( \frac{4 \tan \theta \cos(\theta + \phi)}{3 \sin(\theta + \phi + \delta)} \right) - \left( \frac{2c \cos \phi}{\gamma h \cos \theta \sin(\theta + \phi + \delta)} \right) - \left( \frac{2c_a \cos \phi}{\gamma h \sin(\theta + \phi + \delta)} \right)$$

Optimization of the active earth pressure coefficient \$K\_a\$ is finished for the different \$\theta\_1\$ to \$\theta\_n\$ satisfying the optimization criteria. The optimum value of \$K\_a\$ for \$W'=1.1w\$, \$W'=1.2w\$, \$W'=1.3w\$ are given in Table.1, Table.2, Table 3.

**Table-1**  
**Active earth pressure coefficients (\$K\_a\$) for \$W'=1.1W\$**

\$\phi\$	\$\delta\$	\$C_a\$	\$C=0.1\$	\$C=0.15\$	\$C=0.2\$
			\$K_a\$	\$K_a\$	\$K_a\$
20	0	0	0.399	0.329	0.259
		\$C/2\$	0.365	0.279	0.193
		\$C\$	0.334	0.233	0.134
	\$\phi/2\$	0	0.372	0.294	0.234
		\$C/2\$	0.331	0.254	0.174
		\$C\$	0.311	0.204	0.114
	\$\phi\$	0	0.342	0.276	0.214
		\$C/2\$	0.309	0.223	0.154
		\$C\$	0.289	0.188	0.098
25	0	0	0.319	0.255	0.191
		\$C/2\$	0.288	0.209	0.131
		\$C\$	0.259	0.168	0.077
	\$\phi/2\$	0	0.281	0.234	0.174
		\$C/2\$	0.269	0.189	0.124
		\$C\$	0.231	0.143	0.051
	\$\phi\$	0	0.272	0.213	0.143
		\$C/2\$	0.244	0.167	0.101
		\$C\$	0.217	0.125	0.043

30	0	0	0.251	0.193	0.135
		C/2	0.223	0.152	0.081
		C	0.197	0.114	0.032
	φ/2	0	0.234	0.188	0.114
		C/2	0.201	0.134	0.071
		C	0.177	0.097	0.024
	φ	0	0.213	0.167	0.105
		C/2	0.184	0.114	0.054
		C	0.154	0.081	0.011
35	0	0	0.193	0.141	0.089
		C/2	0.168	0.104	0.04
		C	0.145	0.07	0.002
	φ/2	0	0.177	0.124	0.074
		C/2	0.156	0.094	0.03
		C	0.134	0.067	--
	φ	0	0.159	0.105	0.062
		C/2	0.135	0.077	0.014
		C	0.12	0.042	--
40	0	0	0.145	0.099	0.052
		C/2	0.123	0.066	0.008
		C	0.118	0.035	--
	φ/2	0	0.138	0.067	0.034
		C/2	0.105	0.037	--
		C	0.1	--	--
	φ	0	--	--	--
		C/2	--	--	--
		C	--	--	--

Discussion on results: A detailed parametric study has been conducted to encounter the different of static active earth pressure coefficients for  $W'=1.1w$  with various other parameters like angle of internal friction ( $\phi$ ), wall friction ( $\delta$ ), cohesion ( $c$ ), adhesion ( $c_a$ ). For  $\phi=20^\circ, 25^\circ, 30^\circ, 35^\circ, 40^\circ$ ,  $\delta=0, \phi/2, \phi$ ,  $c=0.1, 0.15, 0.2$ ,  $c_a=0, c/2, c$ .

The profusion of these analysis are shown below.

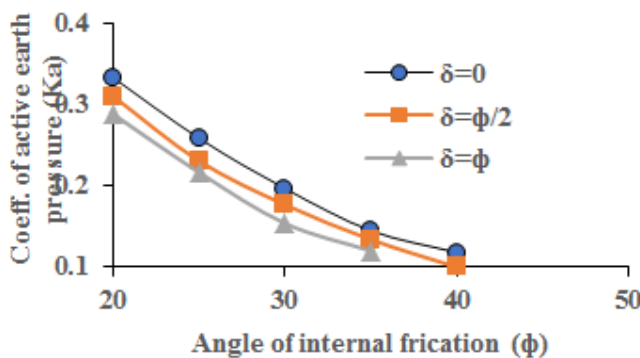


Figure 3 Shows the variation of active earth pressure coefficients with respect to angle of internal friction at different wall friction angles ( $\delta=0, \phi/2, \phi$ ),  $c=0.1, c_a=c$

Figure 3 demonstrates the variation of the active earth pressure coefficient ( $K_a$ ) with angle of internal friction ( $\phi$ ) for

different values of wall friction angle ( $\delta$ ). It shows that the value of  $K_a$  decreases with the rise of angle of internal friction. For example the value of active earth pressure coefficient ( $K_a$ ) for  $\phi=20^\circ$ ,  $\delta=0, \phi/2, \phi$ ,  $c=0.1, c_a=c$  are 0.334, 0.311, 0.281.

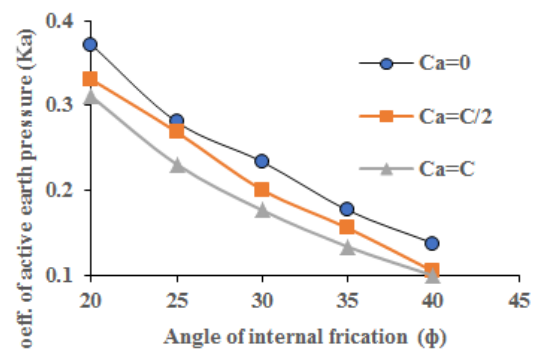


Figure 4 Shows the variation of active earth pressure coefficients with respect to angle of internal friction at different ratio of adhesion parameters ( $c_a=0, c/2, c$ )  $\delta=\phi/2, c=0.1$

Figure 4 demonstrates the variation of the active earth pressure coefficient ( $K_a$ ) with angle of internal friction ( $\phi$ ), for different values of adhesion parameters ( $c_a$ ). It shows that the value of active earth pressure coefficient ( $K_a$ ) decreases with the rise of angle of internal friction ( $\phi$ ). For example the value of  $K_a$  for  $\phi=40$ ,  $c_a=0, c/2, c$  and  $c=0.1, \delta=\phi/2$  are 0.138, 0.105, 0.1.

**Table-2**  
Active earth pressure coefficients ( $K_a$ ) for  $W'=1.2W$

$\phi$	$\delta$	$C_a$	C=0.1	C=0.15	C=0.2
			$K_a$	$K_a$	$K_a$
20	0	0	0.507	0.468	0.431
		C/2	0.477	0.426	0.381
		C	0.449	0.391	0.337
	φ/2	0	0.487	0.443	0.418
		C/2	0.462	0.413	0.352
		C	0.427	0.378	0.302
	φ	0	0.463	0.424	0.387
		C/2	0.441	0.391	0.338
		C	0.403	0.362	0.296
25	0	0	0.454	0.414	0.378
		C/2	0.422	0.371	0.324
		C	0.392	0.332	0.278
	φ/2	0	0.432	0.396	0.361
		C/2	0.402	0.356	0.318
		C	0.376	0.319	0.269
	φ	0	0.415	0.381	0.349
		C/2	0.388	0.343	0.302
		C	0.362	0.309	0.261
		0	0.336	0.306	0.218

30	0	C/2	0.312	0.272	0.236
		C	0.288	0.241	0.199
		0	0.312	0.293	0.254
	$\phi/2$	C/2	0.294	0.261	0.216
		C	0.263	0.217	0.183
		0	0.287	0.258	0.226
	$\phi$	C/2	0.273	0.233	0.198
		C	0.238	0.199	0.173
		0	0.269	0.243	0.219
35	0	C/2	0.247	0.213	0.181
		C	0.226	0.185	0.148
		0	0.247	0.227	0.206
	$\phi/2$	C/2	0.238	0.193	0.169
		C	0.213	0.153	0.134
		0	0.226	0.206	0.173
	$\phi$	C/2	0.219	0.173	0.156
		C	0.196	0.149	0.128
		0	0.212	0.189	0.168
40	0	C/2	0.192	0.162	0.134
		C	0.174	0.138	0.106
		0	--	--	--
	$\phi/2$	C/2	--	--	--
		C	--	--	--
		0	--	--	--
	$\phi$	C/2	--	--	--
		C	--	--	--
		0	--	--	--

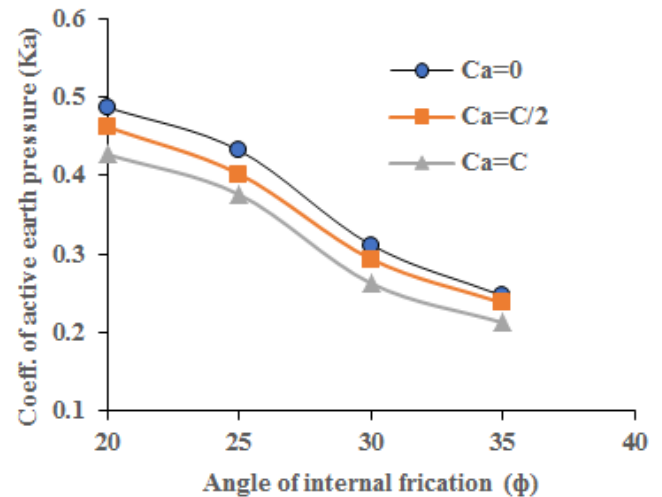


Figure 6 Shows the variation of active earth pressure coefficients with respect to angle of internal friction at different ratio of adhesion parameters ( $c_a=0, c/2, c$ )  $\delta=\phi/2, c=0.1$

**DISCUSSION ON RESULTS:**

A detailed parametric study has been conducted to encounter the different of static active earth pressure coefficients for  $W'=1.2w$  with various other parameters like cohesion( $c$ ) and adhesion( $c_a$ ) for angle of internal friction ( $\phi=20, 25, 30, 35, 40$ ), wall friction angle( $\delta=0, \phi/2, \phi$ ).

The profusion of these analysis are shown below.

Figure 6 demonstrates the variation of the active earth pressure coefficient ( $K_a$ ) with angle of internal friction( $\phi$ ), for different values of adhesion parameters( $c_a$ ). It shows that the value of active earth pressure coefficient( $K_a$ ) decreases with the rise of angle of internal friction( $\phi$ ). For example the value of  $K_a$  for  $\phi=35, c_a=0, c/2, c$  and  $c=0.1, \delta=\phi/2$  are 0.213, 0.153, 0.134.

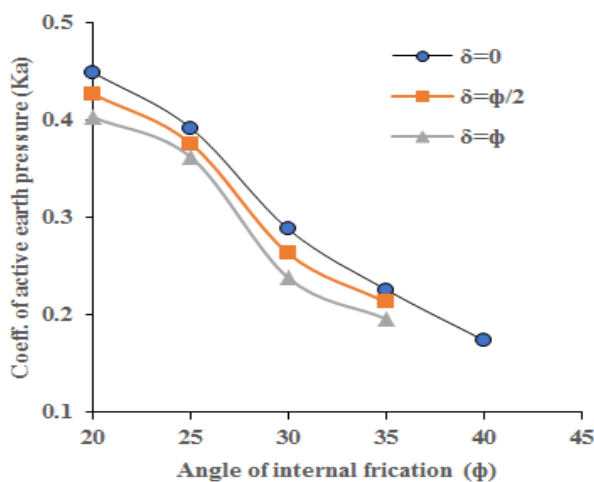


Figure 5 Shows the variation of active earth pressure coefficients with respect to angle of internal friction at different wall friction angles ( $\delta=0, \phi/2, \phi$ ),  $c=0.1, c_a=c$

**Table-3**  
Active earth pressure coefficients ( $K_a$ ) for  $W'=1.3W$

$\phi$	$\delta$	$C_a$	C=0.1	C=0.15	C=0.2
			$K_a$	$K_a$	$K_a$
20	0	0	0.572	0.533	0.496
		C/2	0.542	0.491	0.444
		C	0.498	0.453	0.398
	$\phi/2$	0	0.545	0.528	0.453
		C/2	0.538	0.484	0.421
		C	0.488	0.446	0.372
	$\phi$	0	0.522	0.508	0.434
		C/2	0.517	0.478	0.372
		C	0.477	0.431	0.367
25	0	0	0.469	0.434	0.402
		C/2	0.441	0.396	0.354
		C	0.415	0.362	0.347
	$\phi/2$	0	0.461	0.423	0.371
		C/2	0.431	0.377	0.331
		C	0.401	0.353	0.308
	$\phi$	0	0.441	0.401	0.354
		C/2	0.383	0.362	0.304
		C	0.372	0.331	0.274
0	0	0.381	0.351	0.321	
	C/2	0.356	0.315	0.278	

30	$\phi/2$	C	0.332	0.284	0.239	
		0	0.351	0.323	0.305	
		C/2	0.332	0.286	0.256	
	$\phi$	C	0.327	0.268	0.214	
		0	0.323	0.303	0.284	
		C/2	0.312	0.273	0.234	
35	0	C	0.292	0.232	0.204	
		0	0.305	0.278	0.256	
		C/2	0.283	0.247	0.215	
	$\phi/2$	C	0.262	0.219	0.181	
		0	0.287	0.267	0.235	
		C/2	0.267	0.232	0.204	
	$\phi$	C	0.254	0.203	0.168	
		0	0.265	0.234	0.212	
		C/2	0.251	0.201	0.194	
40	0	C	0.243	0.187	0.148	
		0	0.241	0.218	0.196	
		C/2	0.221	0.189	0.162	
	$\phi/2$	C	0.202	0.164	0.131	
		0	0.232	0.202	0.174	
		C/2	0.217	0.171	0.143	
	$\phi$	C	0.196	-	-	
		0	-	-	-	
		C/2	-	-	-	
			C	-	-	-

**Discussion on results:**

A detailed parametric study has been conducted to encounter the different of static active earth pressure coefficients for  $W=1.3w$  with various other parameters like angle of internal friction ( $\phi$ ), wall friction angle ( $\delta$ ), cohesion ( $c$ ) adhesion ( $ca$ ) for  $\phi=20, 25, 30, 35, 40, \delta=0, \phi/2, \phi$ .

The profusion of these analysis are shown below.

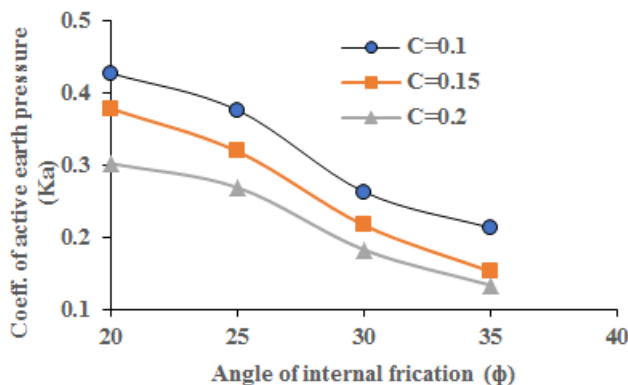


**Figure 7 Shows the variation of active earth pressure coefficients with respect to angle of internal friction at different ratio of cohesion parameters ( $c=0.1, 0.15, 0.2$ ),  $\delta=\phi/2, ca=c$**

Figure 7 demonstrates the variation of the active earth pressure coefficients ( $K_a$ ) with angle of internal friction ( $\phi$ ) for different values of cohesion parameters ( $c$ ). It shows that the value of active earth pressure coefficient ( $K_a$ ) decreases

with the rise of angle of internal friction ( $\phi$ ). For example the value  $K_a$  for  $\phi=20^\circ c=0.1, 0.15, 0.2$  and  $ca=c, \delta=\phi/2$  are 0.311, 0.204, 0.114.

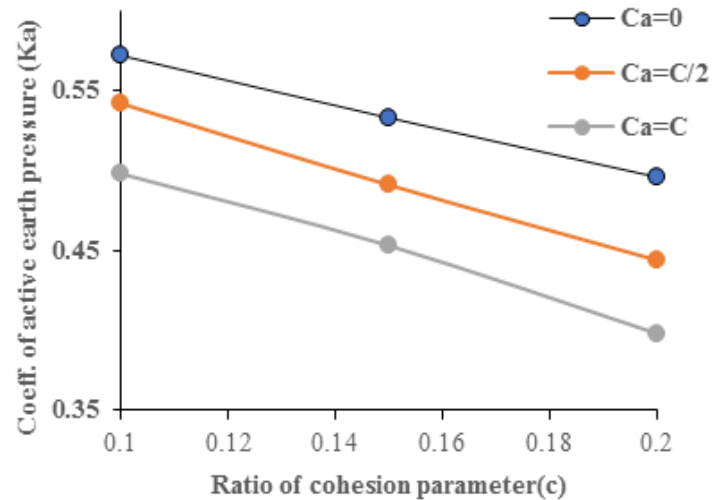


**Figure 8 Shows the variation of active earth pressure coefficients with respect to angle of internal friction at different ratio of adhesion parameters ( $ca=0, c/2, c$ )  $\delta=\phi/2, c=0.1$**

Figure 8 demonstrates the variation of the active earth pressure coefficient ( $K_a$ ) with angle of internal friction ( $\phi$ ), for different values of adhesion parameters ( $ca$ ). It shows that the value of active earth pressure coefficient ( $K_a$ ) decreases with the rise of angle of internal friction ( $\phi$ ). For example the value of  $K_a$  for  $\phi=35, ca=0, c/2, c$  and  $c=0.1, \delta=\phi/2$  are 0.286, 0.266, 0.251.

**CONCLUSION:**

The present review decorates an analytical formulation for the coefficients of all active pressures on the back of the retaining wall supporting against  $C-\phi$  backfill taking into account of weight of wedge, adhesion, cohesion and single rupture angle. Trusting on the obtained analysis, a detailed parametric study is done for the variation of various density of soil and wall parameters. From the point of parametric study it shows the active earth pressure coefficients displays an inverse relation with the rise in angle of internal friction ( $\phi$ ), cohesion ( $c$ ) and adhesion ( $ca$ ). for a specific sequence it may be negative. This shows that there should not be any pressure acting on the retaining wall during active state. On the other hand it increases with the increasing in the density of overburden dumps by 1.1, 1.2, 1.3 times of natural density of soil.

**REFERENCES:**

- [1] Jadar, C.M and Ghosh., (2017) ‘Seismic bearing capacity of shallow strip footing using horizontal slice method’, Indian Geotechnical Engineering 11(1), 38-50.
- [2] Askari, F. and Farzaneh, O., (2003), ‘Upper – bound solutions for seismic bearing capacity of shallow foundations near slopes’, Geotechnique 53, No. 8, 697-702.
- [3] Budhu, M. and Al-Karni, A., (1993) ‘Seismic bearing capacity of soils’, Geotechnique, 43(1), 181-187
- [4] Choudhury, D. and Nimbalkar, S. S., (2006), ‘Pseudo dynamic approach of seismic active earth pressure behind retaining wall’, Geotechnical and Geological Engineering, Springer, 24, 1103-1113.
- [5] Choudhury, D. and Nimbalkar, S. S., (2005), ‘Seismic passive resistance by pseudo-dynamic method’, Geotechnique, 55, 699-702.
- [6] Choudhury, D. and Subba Rao, K. S., (2005), ‘Seismic bearing capacity of shallow strip footings’, Geotechnical and Geological Engineering, Springer, 23, 403-418
- [7] Choudhury, D. and Subba Rao, K. S., (2006), ‘Seismic bearing capacity of shallow strip footings embedded in slope’, International Journal of Geomechanics, ASCE, vol.(6), 176-184
- [8] Coulomb, C. A., (1776), ‘Essai sur une application des règles de maximées et minimis a quelques problèmes de statique relatifs a l’architecture’, Memories de Mathematique et de Physique, Presents a l’Academic Royele des Sciences Par divers Savans et lus dans ses Assemblees, Paris, vol.7
- [9] Basha,M. and Babu,S.(2008) “Reliability Based Design Optimization of Bridge Abutments Using Pseudo-dynamic Method”.
- [10] Choudhury, D. and Nimbalkar, S. S., (2005), ‘Pseudo dynamic approach of seismic active earth pressure behind retaining wall’, Geotechnical and Geological Engineering, Springer, 24, 1103-1113.
- [11] Choudhury, D. and Subba Rao, K. S. (2002), "Seismic passive resistance in soils for negative wall friction." Can. Geotech. J., Ottawa, 39, 971-981.
- [12] Choudhury,D.(2004)" seismic passive resistance at soil wall interference " ,pg no 2746.
- [13] Dewoolkar, M et al.(2000) “Experimental developments for studying static and seismic behavior of retaining walls with liquafiable backfills.” Architecture engineering , CO 80309-
- [14] Ghanbari, A. and Ahmadabadi, M., (2010), “Pseudo dynamic active earth pressure analysis of inclined retaining walls using horizontal slices method”, Transaction A; Civil Engineering, ScientiaIranica, vol. 17, No. 2.
- [15] Ghosh,S . and Senguptha,S.(2012),”Formulation of Seismic Passive Resistance of Non-Vertical Retaining Wall Backfilled with c-Φ Soil”.
- [16] Giri,D.(2013) “Pseudo-dynamic methods for seismic passive earth pressure behind a cantilever retaining wall with inclined backfill”, Geomechanics and Geoengineering, 9:1, 72-78.
- [17] Kumar,K. and Ghosh,S.(2014) “Non-linear failure surface analysis of seismic active earth pressure on retaining wall considering Rayleigh waves”. Geotechnical Engineering, 10:5, 476-4.
- [18] Ling, H. et al. (2009) “Seismic Response of Geocell Retaining Walls: Experimental Studies.” Geotechnical engineering.
- [19] Subba rao,K et al.(2005) “Seismic Passive Earth Pressures in Soils.”